


Association Between Amyloid and Tau Accumulation in Young Adults With Autosomal Dominant Alzheimer Disease

Yakeel T. Quiroz, PhD; Reisa A. Sperling, MD; Daniel J. Norton, PhD; Ana Baena, BA; Joseph F. Arboleda-Velasquez, MD, PhD; Danielle Cosio, BS; Aaron Schultz, PhD; Molly Lapoint, BS; Edmarie Guzman-Velez, PhD; John B. Miller, MD; Leo A. Kim, MD, PhD; Kewei Chen, PhD; Pierre N. Tariot, MD; Francisco Lopera, MD; Eric M. Reiman, MD; Keith A. Johnson, MD

 Editorial page 536

IMPORTANCE It is critically important to improve our ability to diagnose and track Alzheimer disease (AD) as early as possible. Individuals with autosomal dominant forms of AD can provide clues as to which and when biological changes are reliably present prior to the onset of clinical symptoms.

OBJECTIVE To characterize the associations between amyloid and tau deposits in the brains of cognitively unimpaired and impaired carriers of presenilin 1 (*PSEN1*) E280A mutation.

DESIGN, SETTING, AND PARTICIPANTS In this cross-sectional imaging study, we leveraged data from a homogeneous autosomal dominant AD kindred, which allowed us to examine measurable tau deposition as a function of individuals' proximity to the expected onset of dementia. Cross-sectional measures of carbon 11-labeled Pittsburgh Compound B positron emission tomography (PET) and flortaucipir F 18 (previously known as AV 1451, T807) PET imaging were assessed in 24 *PSEN1* E280A kindred members (age range, 28-55 years), including 12 carriers, 9 of whom were cognitively unimpaired and 3 of whom had mild cognitive impairment, and 12 cognitively unimpaired noncarriers.

MAIN OUTCOMES AND MEASURES We compared carbon 11-labeled Pittsburgh Compound B PET cerebral with cerebellar distribution volume ratios as well as flortaucipir F 18 PET cerebral with cerebellar standardized uptake value ratios in mutation carriers and noncarriers. Spearman correlations characterized the associations between age and mean cortical Pittsburgh Compound B distribution volume ratio levels or regional flortaucipir standardized uptake value ratio levels in both groups.

RESULTS Of the 24 individuals, the mean (SD) age was 38.0 (7.4) years, or approximately 6 years younger than the expected onset of clinical symptoms in carriers. Compared with noncarriers, cognitively unimpaired mutation carriers had elevated mean cortical Pittsburgh Compound B distribution volume ratio levels in their late 20s, and 7 of 9 carriers older than 30 years reached the threshold for amyloidosis (distribution volume ratio level > 1.2). Elevated levels of tau deposition were seen within medial temporal lobe regions in amyloid-positive mutation carriers 6 years before clinical onset of AD in this kindred. Substantial tau deposition in the neocortex was only observed in 1 unimpaired carrier and in those with mild cognitive impairment. β -Amyloid uptake levels were diffusely elevated in unimpaired carriers approximately 15 years prior to expected onset of mild cognitive impairment. In carriers, higher levels of tau deposition were associated with worse performance on the Mini-Mental State Examination (entorhinal cortex: $r = -0.60$; $P = .04$; inferior temporal lobe: $r = -0.54$; $P = .06$) and the Consortium to Establish a Registry for Alzheimer Disease Word List Delayed Recall (entorhinal cortex: $r = -0.86$; $P < .001$; inferior temporal lobe: $r = -0.70$; $P = .01$).

CONCLUSIONS AND RELEVANCE The present findings add to the growing evidence that molecular markers can characterize biological changes associated with AD in individuals who are still cognitively unimpaired. The findings also suggest that tau PET imaging may be useful as a biomarker to distinguish individuals at high risk to develop the clinical symptoms of AD and to track disease progression.

JAMA Neurol. 2018;75(5):548-556. doi:10.1001/jamaneurol.2017.4907
Published online February 12, 2018.

Author Affiliations: Author affiliations are listed at the end of this article.

Corresponding Author: Yakeel T. Quiroz, PhD, Massachusetts General Hospital, Harvard Medical School, 149 13th St, Office 10.014, Boston, MA 02129 (yquiroz@mgh.harvard.edu).

Alzheimer disease (AD) is defined at the neuropathological molecular level by amyloid plaques and neurofibrillary tangles.^{1,2} This neuropathology generally follows a characteristic spatial distribution, with amyloid plaques beginning in neocortical association regions and tangles beginning in the medial temporal lobe and then spreading into adjacent association cortices with subsequent pancortical extension.^{3,4}

Presenilin 1 (*PSEN1*; OMIM, 104311) mutations predispose individuals to develop autosomal dominant Alzheimer disease (ADAD), usually relatively early in adulthood.⁵ While the pathogenesis of ADAD may be different from late-onset AD (LOAD) and some clinical features may differ, these conditions are markedly similar in terms of their biological profiles, including abnormalities in amyloid biomarkers, brain structure, and brain activity.⁶ Biomarker investigations of families with ADAD have already shed light on the trajectory of AD-related brain changes, especially prior to the onset of clinical symptoms.⁶⁻⁸ In addition, ongoing studies of these families will inform the design of future prevention clinical trials for individuals at risk for AD.

We used brain imaging and other biomarker measures to detect changes in preclinical *PSEN1* E280A (Glu280Ala) mutation carriers from the largest known ADAD kindred. Residing in Antioquia, Colombia, this kindred is estimated to have approximately 5000 living members, including approximately 1800 mutation carriers.⁹ Approximately 30% of living mutation carriers from this kindred are currently experiencing symptoms of AD, with median ages of 44 years (95% CI, 43-45) at onset of mild cognitive impairment (MCI) and 49 years (49-50) at onset of dementia.⁹ These carriers show evidence of preclinical AD in the years and decades before their estimated clinical onset, including elevated cortical amyloid levels, lower cerebral metabolic rates for glucose, smaller hippocampal volumes, lower cerebrospinal fluid β -amyloid (A β) 1-42 levels, higher cerebrospinal fluid total tau and tau phosphorylated at threonine 181 levels, and higher plasma A β 1-42 measurements.⁶ In fact, even children and young adults with *PSEN1* E280A mutations have alterations in magnetic resonance imaging measurements of brain structure^{7,10} and function (eg, hippocampal hyperactivation and less precuneus deactivation) more than 2 decades prior to the kindred's median age of MCI onset.^{7,10}

Recently, it has become possible to investigate the aggregation of tau in vivo using positron emission tomography (PET) imaging. This novel biomarker holds promise for detecting AD in the preclinical stage. Examination of tau PET in ADAD is particularly relevant to understanding the aggregation and spreading of tau in AD without the major confounders of aging and comorbidities that often exist in sporadic AD. Additionally, the study of tau PET in combination with Pittsburgh Compound B (PiB) PET measures can reveal the extent to which amyloid-tau relations in ADAD differ from those seen in sporadic AD. To our knowledge, tau imaging has not been extensively tested in ADAD to date.

In this study, we used PET imaging to characterize amyloid burden and tau accumulation as well as the association between the 2 in the brains of young *PSEN1* E280A mutation

Key Points

Question Does cortical β -amyloid deposition precede tau tangle formation within and beyond the medial temporal lobe in individuals with autosomal dominant Alzheimer disease?

Findings In this cross-sectional study that included 24 members of a Colombian kindred with autosomal dominant Alzheimer disease, elevated tau levels were seen in regions of the medial temporal lobe in unimpaired presenilin 1 E280A mutation carriers in their late 30s, and significant tau tangle formation in neocortical regions was observed in 1 cognitively unimpaired carrier as well as in those with mild cognitive impairment.

Meaning These findings add to the growing evidence that tau positron emission tomography imaging may be useful to characterize biological changes associated with Alzheimer disease in cognitively unimpaired individuals and to track disease progression.

carriers. We hypothesized that, similar to what has been reported in individuals with LOAD,¹¹ *PSEN1* mutation carriers would have abnormal levels of A β before evidence of tau tangle formation as measured by PET imaging both within and beyond the medial temporal lobe.

Methods

Study Design and Participants

This cross-sectional study collected PET images using 2 radioligands, flortaucipir F 18 (18F FTP; previously known as AV 1451, T807), which selectively binds tau aggregates, and carbon 11-labeled PiB, which selectively binds amyloid deposits, in individuals with and without the *PSEN1* E280A mutation. These images were compared with each other and with neuropsychological data. Volunteers were recruited from the Colombian Alzheimer Prevention Initiative registry, which currently includes more than 5000 living members of the *PSEN1* E280A kindred. The participants selected for the present study, both carriers and noncarriers, descended from a common ancestor, and their ages ranged from 28 to 55 years. Only participants living in the metropolitan area of the Aburra Valley within 105 miles of the University of Antioquia, Medellin, Antioquia, Colombia, were invited to participate in the study. Potential participants were screened in advance for the presence of neurological and psychiatric disorders, drug use, and eligibility to undergo magnetic resonance imaging. Participants provided written informed consent before enrollment into study procedures. Participants were studied under guidelines approved by local institutional review boards. Ethics approval was obtained from the University of Antioquia Ethics Committee for procedures undertaken in Colombia and the Massachusetts General Hospital Institutional Review Board for procedures undertaken in the United States. All data were acquired by investigators who were masked to the participants' genetic status.

Cognitively unimpaired participants had to show no cognitive impairment on a standard cognitive battery, including

a clinical diagnostic rating scale (CDR) score of 0 and a Folstein Mini-Mental State Examination score of 26 or greater. Symptomatic mutation carriers were required to have a CDR score of 0.5 and MCI due to AD according to National Institute on Alcohol Abuse and Alcoholism criteria.¹² Cognitively unimpaired mutation carriers and noncarriers were matched for sex, age, and education. A cohort of 9 cognitively unimpaired individuals, 3 cognitively impaired mutation carriers with MCI, and 12 age-matched noncarriers traveled to Boston, Massachusetts, in the United States for PET imaging.

Procedures

All clinical measures were undertaken at the University of Antioquia, and PET scanning was performed at the Massachusetts General Hospital, Boston, Massachusetts. Neurocognitive testing included the Mini-Mental State Examination, CDR, and a Spanish version of the Consortium to Establish a Registry for Alzheimer Disease (CERAD) battery, which was adapted to this Colombian population.¹³ Additional testing consisted of the Yesavage Geriatric Depression Scale¹⁴ and the Functional Assessment Staging test,¹⁵ which were performed during screening and at baseline before imaging, respectively. Testing was conducted in Spanish by neuropsychologists or by psychologists trained in neuropsychological assessment. Clinical history and neurological examination were performed by a neurologist or by a physician trained in the assessment of neurodegenerative disorders. Clinical data were recorded on a relational database at the Grupo de Neurociencias, Universidad de Antioquia, Medellin, Antioquia, Colombia.

Image Acquisition and Processing

Flortaucipir F 18 was prepared at Massachusetts General Hospital with a mean (SD) radiochemical yield of 14% (3%) and a mean (SD) specific activity of 216 (60) GBq/ μ mol at the end of synthesis (60 min) and was validated for human use.¹⁶ Carbon 11-labeled PiB was prepared and PET images were acquired as described previously.¹⁷ All PET images were acquired using a Siemens/CTI ECAT PET HR scanner (3-dimensional mode; 63 image planes; 15.2-cm axial field of view; 5.6-mm transaxial resolution; and 2.4-mm slice interval). Carbon 11-labeled PiB PET was acquired with a 8.5- to 15.0-mCi bolus injection followed immediately by a 60-minute dynamic acquisition in 69 frames (12×15 seconds, 57×60 seconds). Flortaucipir F 18 was acquired from 80 to 100 minutes after a 9.0- to 11.0-mCi bolus injection in 4×5 -minute frames. Positron emission tomography images were reconstructed and attenuation-corrected, and each frame was evaluated to verify adequate count statistics and absence of head motion. All imaging was done within the span of 1 week. Cognitive testing was conducted within 2 months of imaging acquisitions.

Magnetic resonance imaging was performed on a MAGNETOM Tim Trio 3-T scanner (Siemens) and included a magnetization-prepared rapid gradient-echo processed with FreeSurfer image analysis suite version 5.0 to identify gray and white matter and pial surfaces to permit region of interest (ROI) parcellation for cerebellar gray matter, hippocampus, and the following Braak stage-related cortices: entorhinal, parahip-

pocampal, inferior temporal, fusiform, and posterior cingulate, as described previously.^{11,17-19}

To evaluate the anatomical distribution of cortical FTP binding, each individual PET data set was rigidly coregistered to the individual's magnetization-prepared rapid gradient-echo magnetic resonance data using statistical parametric mapping (SPM8; Wellcome Trust Centre for Neuroimaging). The cortical ribbon and subcortical ROIs defined by magnetic resonance imaging as described above were transformed into the PET native space; PET data were sampled within each right-left ROI pair. Standardized uptake value ratio (SUVR) values were represented graphically on vertices at the pial surface. Positron emission tomography data were not partial volume corrected.

Flortaucipir F 18-specific binding was expressed in FreeSurfer ROIs as the SUVR to cerebellum, similar to a previous report,¹¹ using the FreeSurfer cerebellar gray matter ROI as the reference. For voxelwise analyses, each individual's magnetization-prepared rapid gradient-echo was registered to the template magnetic resonance in SPM8, and the spatially transformed SUVR PET data were smoothed with a 8-mm Gaussian kernel to account for individual anatomic differences.²⁰ To account for possible 18F FTP off-target binding in choroid plexus, which may confound hippocampal signal, we used a linear regression to regress the choroid plexus, as previously reported.²¹

Carbon 11-labeled PiB PET data were expressed as the distribution volume ratio (DVR) with cerebellar gray matter as the reference tissue; regional time-activity curves were used to compute regional DVRs for each ROI using the Logan graphical method²² applied to data from 40 to 60 minutes after injection.¹⁷ Carbon 11-labeled PiB retention was assessed using a large cortical ROI aggregate that included frontal, lateral temporal, and retrosplenial cortices, as described previously.^{23,24}

Statistical Analyses

Flortaucipir F 18 SUVRs in mutation carriers and noncarriers were compared both voxelwise and within FreeSurfer-defined ROIs. The Mann-Whitney *U* test was used to compare PET ROI measures between groups. Positron emission tomography ROI measures in each group were correlated with age using Spearman rho. Carbon 11-labeled PiB frontal, lateral temporal, and retrosplenial cortices were used as a continuous measure of A β levels, and amyloid-positive was defined as a DVR greater than 1.2 in the frontal, lateral temporal, and retrosplenial cortices.²⁵ Correlations between mean cortical PiB and inferior temporal 18F FTP measures as well as relationships with age and neuropsychological test scores were evaluated with Spearman rho.

Results

Demographic Information

Table 1 shows participant demographic characteristics, including clinical ratings and cognitive test scores. The cognitively unimpaired mutation carrier and noncarrier groups did not differ significantly in their age, sex, education, or neuropsychological

Table 1. Demographic Characteristics

Characteristic	Mean (SD)			P Value ^a
	Presenilin 1 E280A Mutation Carriers			
	MCI (n = 3)	Unimpaired (n = 9)	Noncarriers (n = 12)	
Age, y	43.83 (1.15)	34.33 (5.49)	39.44 (8.62)	.19
Education, y	9.67 (4.16)	9.00 (3.43)	10.33 (4.23)	.51
MMSE score	24.33 (5.51)	28.44 (1.33)	29.08 (0.52)	.31
CERAD Word List score				
Immediate Learning	12.67 (5.69)	18.78 (4.71)	21.75 (3.36)	.25
Delayed Recall	3.00 (3.61)	6.11 (2.71)	7.83 (1.03)	.22
Semantic fluency (animals) score	19.33 (5.51)	21.44 (5.81)	20.92 (3.68)	.86

Abbreviations: CERAD, Consortium to Establish a Registry for Alzheimer Disease; MCI, mild cognitive impairment; MMSE, Mini-Mental State Examination.

^a P value as defined by an independent-samples Mann-Whitney U test for presenilin 1 unimpaired mutation carriers vs noncarriers.

Table 2. Flortaucipir F 18 Binding in Regions of Interest Comparing Presenilin 1 Mutation Carriers With Noncarriers

Region of Interest	Mean (SD)			P Value ^a
	Presenilin 1 E280A Mutation Carriers			
	MCI (n = 3)	Unimpaired Carriers (n = 9)	Noncarriers (n = 12)	
PIB DVR	1.53 (0.06)	1.21 (0.14)	1.04 (0.02)	.001
Hippocampus	1.67 (0.17)	1.30 (0.30)	1.13 (0.09)	.17
Entorhinal	1.59 (0.25)	1.20 (0.33)	1.01 (0.06)	.08
Parahippocampal	1.49 (0.23)	1.18 (0.21)	1.03 (0.05)	.03
Inferior temporal	1.42 (0.34)	1.14 (0.10)	1.12 (0.07)	.60

Abbreviations: DVR, distribution volume ratio; MCI, mild cognitive impairment; PIB, Pittsburgh Compound B.

^a P value as defined by an independent-samples Mann-Whitney U test for presenilin 1 unimpaired mutation carriers vs noncarriers.

logical test scores. Compared with unimpaired mutation carriers, cognitively impaired mutation carriers were older and had significantly lower neuropsychological test scores.

Carbon 11-Labeled PiB DVR in *PSEN1* Mutation Carriers

No elevated amyloid accumulation was seen in any noncarriers, as expected (PiB DVR < 1.1 in all individuals). The youngest mutation carrier, aged 28 years, showed no PIB elevation (PiB = 1.02), but beginning at age 29 years, mutation carriers showed elevated PiB uptake (PiB DVR > 1.1 in all but 1 individual). Seven of 9 mutation carriers 30 years and older reached the threshold for amyloid positivity. Mutation carriers with MCI had the highest PiB DVR values (mean [SD], 1.53 [0.06]; 95% CI, -0.57 to -0.44), followed by unimpaired mutation carriers (mean [SD], 1.21 [0.14]; 95% CI, -0.24 to -0.08), who in turn showed higher carbon 11-labeled PiB DVR than noncarriers (mean [SD], 1.04 [0.02]; $P < .001$). The cerebral pattern of A β deposition resembled that found in clinically affected individuals who are at risk for LOAD.²⁶ This includes preferential PiB binding in the posterior cingulate, precuneus, parietotemporal, frontal, and basal ganglia regions.

Given the possible confounders of using the cerebellum as the reference region,^{27,28} we also performed the PiB and FTP analyses using white matter as a reference. Results with white matter were very similar to the results using the cerebellum (eg, the statistical differences observed with cerebellum as the reference region were also observed with white matter as the reference).

Regional 18F FTP Binding in *PSEN1* Mutation Carriers

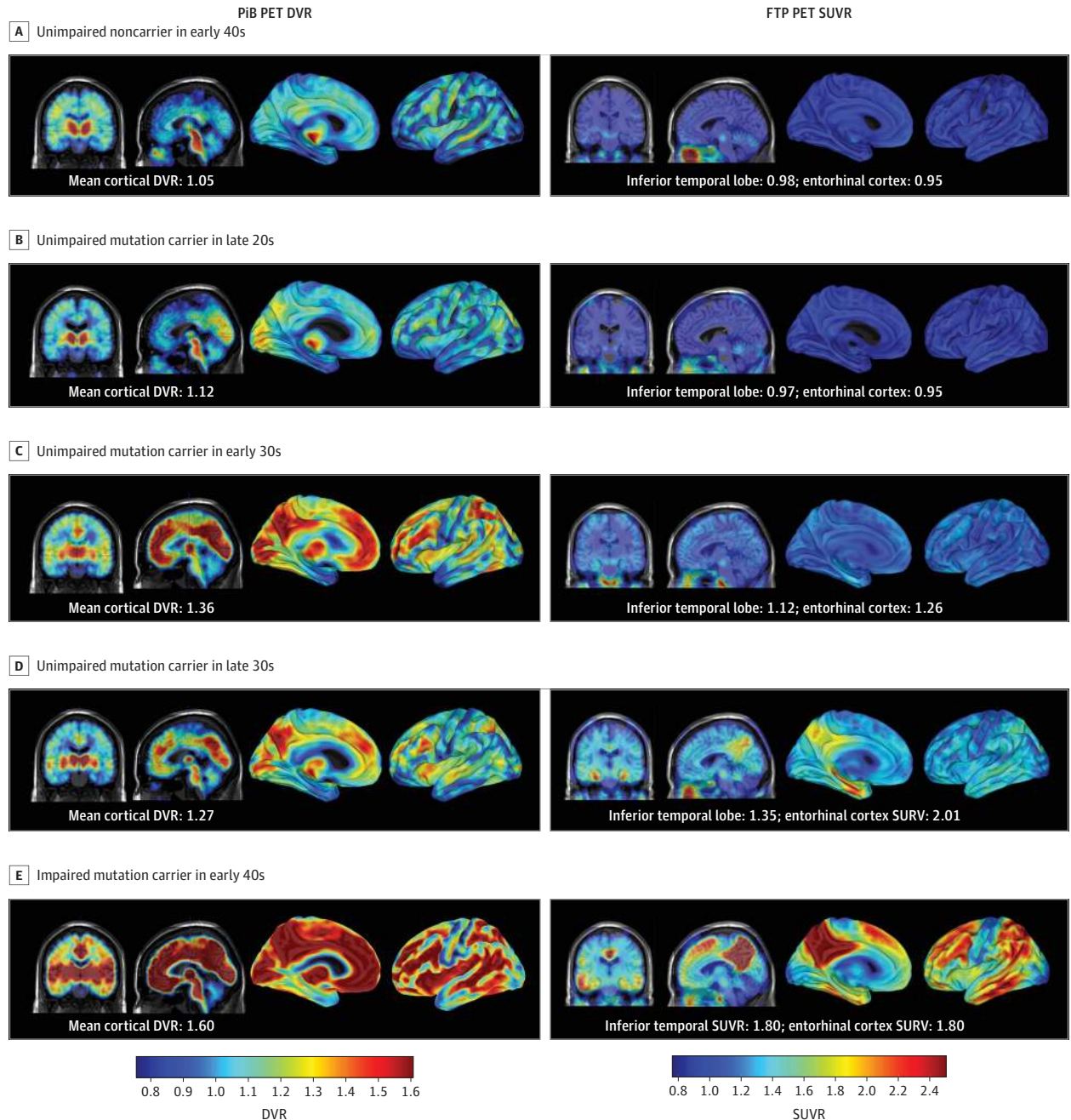
Table 2 shows the FTP binding in ROIs comparing mutation carriers with noncarriers. Regional FTP binding is shown in

representative individuals in **Figure 1**, and group comparisons are shown in **Figure 2**. Compared with noncarriers, the group of *PSEN1* mutation carriers had elevated 18F FTP SUVRs in the entorhinal cortex (mean [SD] SUVR, 1.29 [0.33] vs 1.01 [0.05]; mean difference, -0.28; 95% CI, -0.43 to -0.04; $P = .01$), hippocampus (mean [SD] SUVR, 1.37 [0.30] vs 1.12 [0.08]; mean difference, -0.25; 95% CI, -0.49 to -0.03; $P = .03$), and parahippocampal gyrus (mean [SD] SUVR, 1.25 [0.23] vs 1.03 [0.05]; mean difference, -0.22; 95% CI, -0.34 to -0.05; $P = .004$) (Figure 2). The subgroup of unimpaired carriers also had elevated mean FTP SUVRs in medial temporal regions, but they differed significantly from noncarriers only in parahippocampal gyrus (mean [SD] SUVR, 1.18 [0.21] vs 1.03 [0.05]; mean difference, -0.15; 95% CI, -0.21 to 0.00; $P = .03$). Individual threshold-based anatomic assessments showed that unimpaired carriers with the highest PiB DVR values also had the highest FTP binding in the medial temporal lobe and inferior temporal regions. In patients with MCI, FTP binding was elevated in widespread neocortical regions, most prominently in inferior and lateral temporo-parietal, parieto-occipital, and posterior cingulate/precuneus regions (Figure 1).

Associations Among PET Measures, Age, and Cognitive Measures

In mutation carriers, greater age was associated with both higher cortical PiB DVR ($r = 0.88$; $P < .001$) and higher 18F FTP SUVR binding in the hippocampus ($r = 0.70$; $P = .01$), entorhinal cortex ($r = 0.81$; $P = .02$), parahippocampal gyrus ($r = 0.74$; $P = .006$), and inferior temporal ($r = 0.74$; $P = .007$) regions (Figure 3). No such relationships were significant in noncarriers. In mutation carriers, greater entorhinal and inferior temporal lobe 18F FTP SUVR values were associated

Figure 1. Spatial Patterns of Carbon 11-Labeled Pittsburgh Compound B (PiB) Positron Emission Tomography (PET) and Flortaucipir F 18 (FTP) PET Binding in Presenilin 1 E280A Mutation Carriers



Coronal and sagittal PiB PET distribution volume ratio (DVR) maps are shown on the left, and coronal and sagittal FTP PET standardized uptake value ratio (SUVR) maps are presented on the right. Images are displayed in standardized atlas space, along with whole-brain surface renderings, with a left hemisphere view. A, An unimpaired noncarrier in their early 40s with low β -amyloid ($A\beta$) levels and low FTP binding in the inferior temporal cortex. B, An unimpaired mutation carrier in their late 20s with low $A\beta$ levels and low FTP binding in the inferior temporal cortex. C, An unimpaired mutation carrier in their early 30s with higher $A\beta$ levels and low, nonspecific FTP binding in the inferior temporal

lobe. D, An unimpaired mutation carrier in their late 30s with high $A\beta$ and tau levels with FTP binding in the inferior temporal and parietal cortices.

E, An impaired mutation carrier in their early 40s with mild cognitive impairment with high $A\beta$ levels and extensive FTP binding in the temporal, parietal, and frontal cortices. Elevated levels of FTP binding are evident within medial temporal lobe regions in amyloid-positive mutation carriers within 10 years of estimated years to symptom onset. Substantial FTP binding in the neocortex is evident in mutation carriers with the highest levels of $A\beta$.

with worse performance on the Mini-Mental State Examination (entorhinal cortex: $r = -0.60$; $P = .04$; inferior temporal

lobe: $r = -0.54$; $P = .06$) and the CERAD Word List Delayed Recall (entorhinal cortex: $r = -0.86$; $P < .001$; inferior tempo-

ral lobe: $r = -0.70$; $P = .01$). Greater inferior temporal tau was also related to worse performance on the CERAD Word List Immediate Learning ($r = -0.74$; $P = .006$). Greater PiB binding was only associated with CERAD Word List Delayed Recall ($r = -0.70$; $P = .01$).

18F FTP and PiB Binding in Relation to Each Other

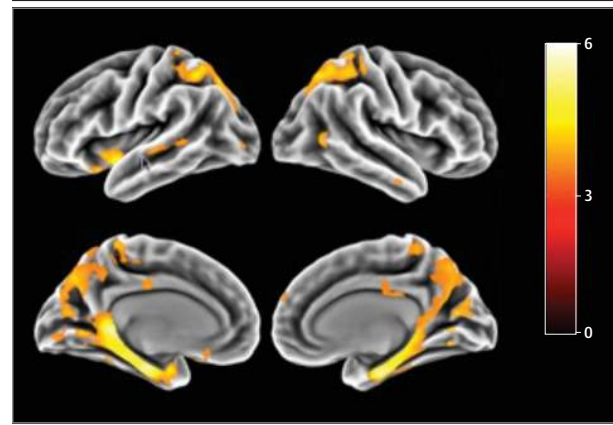
Inferior temporal lobe 18F FTP binding was associated with higher mean cortical PiB retention in mutation carriers ($r = 0.67$; $P = .02$). In our sample, elevated levels of PiB uptake began around age 30 years. Elevated levels of tau were not observed in mutation carriers younger than 38 years. At this stage, tracer retention was only observed in the entorhinal cortex, and with increasing age of the carrier, higher tau levels were also observed in the inferior temporal and lateral temporal lobe. Flortaucipir F 18 binding in the neocortex was observed in 1 cognitively unimpaired carrier aged 38 years and in all cognitively impaired individuals.

Discussion

In this study, we characterized the spatial pattern and temporal lag cross-sectionally of tau and amyloid deposition in the brains

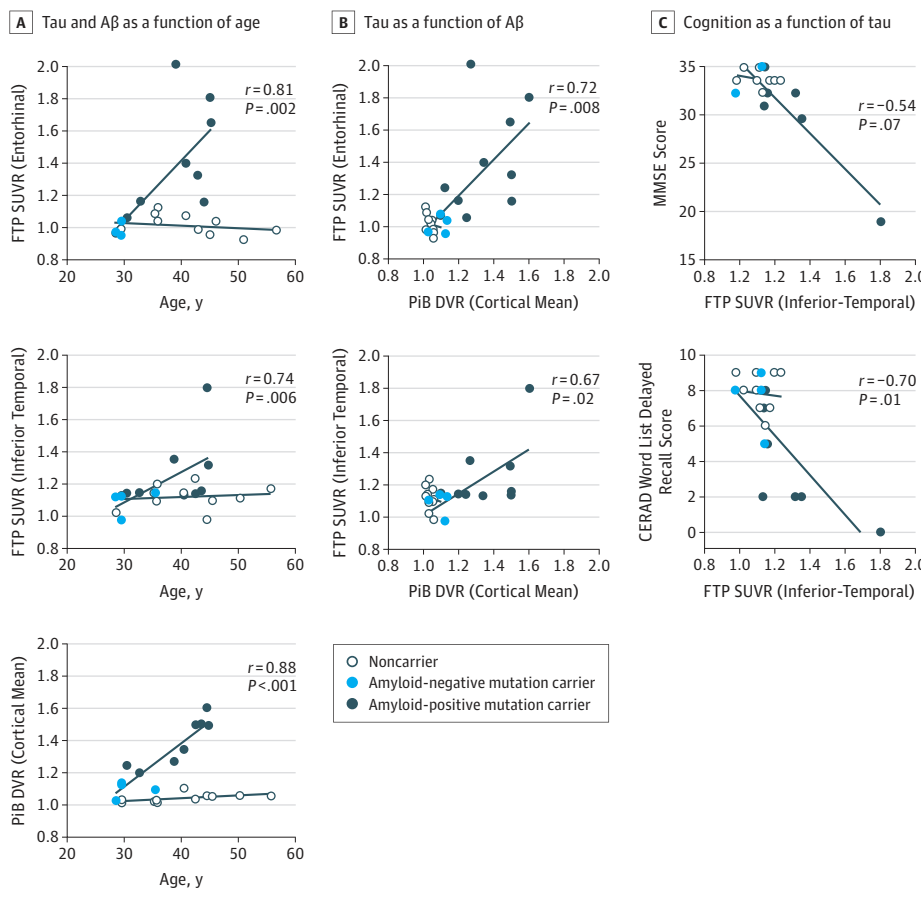
of 24 *PSEN1* E280A mutation carriers and noncarriers from the largest known kindred with ADAD. We used PET images with 2 radioligands, 18F FTP, which selectively binds tau aggregates, and carbon 11-labeled PiB, which selectively binds amyloid deposits. Elevated levels of FTP binding were seen within medial

Figure 2. Comparison of Spatial Distribution of Flortaucipir F 18 Binding Between the 12 Presenilin 1 Carriers and the 12 Noncarriers



The threshold of significance was $P < .001$.

Figure 3. Relations Among Flortaucipir F 18 (FTP) Standardized Uptake Value Ratios (SUVRs) and Related Variables in Presenilin 1 Mutation Carriers and Noncarriers



A, Tau and β -amyloid ($A\beta$) levels as a function of age. B, Tau level as a function of $A\beta$ level. C, Cognition as a function of tau level. Open circles indicate noncarriers from the *PSEN1* kindred, light blue circles indicate *PSEN1* amyloid-negative mutation carriers (distribution volume ratio [DVR] < 1.2), and dark blue circles indicate *PSEN1* amyloid-positive mutation carriers (DVR > 1.2). A single carrier had a DVR level of 1.195 and is shown as a dark blue circle, despite being amyloid negative according to convention. Linear fit lines are shown for carriers and noncarriers separately to aid inspection. CERAD indicates Consortium to Establish a Registry for Alzheimer Disease; DVR, distribution volume ratio; MMSE, Mini-Mental State Examination; PiB, Pittsburgh Compound B.

temporal lobe regions in amyloid-positive mutation carriers 6 years before clinical onset. β -Amyloid uptake levels were diffusely elevated in unimpaired carriers approximately 15 years prior to expected onset of MCI, consistent with our previous report²⁹ of increased mean cortical 18F florbetapir SUVR levels in individuals from the same kindred. Furthermore, 18F FTP SUVR levels were correlated with clinical measures.

We leveraged data from a large, homogeneous ADAD kindred with a single-gene mutation with well-characterized ages at the onset of MCI (mean [SD] age, 44 [5] years) and dementia (mean [SD] age, 49 [5] years). Studies of *PSEN1* mutation carriers allow us to examine cognitively unimpaired individuals who will go on to develop AD in the future with virtual certainty. Previously, we showed that unimpaired mutation carriers from this kindred had significantly lower cerebral metabolic rates for glucose, smaller hippocampal volumes, lower cerebrospinal fluid A β 1-42 measurements, higher cerebrospinal fluid total tau and tau phosphorylated at threonine 181 levels, and higher plasma A β 1-42 measurements.⁶ To our knowledge, the present study is the first to investigate tau aggregation using PET imaging in this kindred. The homogeneity of disease course in these mutation carriers allowed us to observe tau and A β deposition as a function of individuals' proximity to the expected onset of MCI and dementia. With respect to amyloid, the present findings confirm that A β burden in the preclinical stages of ADAD has a similar spatial distribution as in LOAD and begins more than a decade before the onset of clinical symptoms.^{29,30} With respect to tau, elevated levels of FTP binding in medial temporal lobe regions were only observed in individuals who already showed substantial A β deposition in cortical regions. Tau aggregation in the neocortex was observed in individuals with early MCI, consistent with the hypothesis that tau's spread beyond the medial temporal lobe is temporally coupled with cognitive impairment.¹³ The lack of apparent tau deposition in the neocortex until roughly 6 years prior to MCI combined with the diffuse spatial profile of tau deposition in patients with MCI suggests that tau spreads rapidly once it begins to aggregate in the cortex.

The other major PET study of preclinical ADAD is being conducted by the Dominantly Inherited Alzheimer Network (DIAN) group. This study reported PiB data in ADAD in individuals with various AD-causing mutations³¹ and has begun to report data on FTP in these individuals.³³ Overall, the results from the Colombia kindred agree with those from DIAN for both FTP and PiB imaging. With respect to A β , DIAN showed that, averaging across mutations, individuals with preclinical ADAD showed diffuse cortical PiB elevation years before the estimated age of onset for each individual's family.^{31,32} This result is consistent with the present study and another one based on the Colombian kindred,⁶ both of which showed that PiB levels begin to be elevated approximately 15 years prior to estimated onset of MCI. With respect to tau, DIAN has presented preliminary findings, including 11 carriers of various AD-causing mutations³³ and 63 individuals in a study that included LOAD.³⁴ This study as well as the present study found that tau deposition in ADAD had a similar spatial pro-

file compared with LOAD. The DIAN study also reported an intriguing difference between ADAD and LOAD, where greater tau aggregation was present in individuals with ADAD with a CDR of 0.5 compared with individuals with LOAD with the same CDR.³⁴ It is unclear how reliable that trend is because the number of participants with CDR of 0.5 in that comparison were not reported in the DIAN presentations. Further, in LOAD, there was notable interindividual variability in tau extension at that CDR.¹³ Given the sparse data on tau in LOAD and in both major ADAD studies, it is unclear whether differences in the spatial distribution of tau may be associated with particular mutations and not others.

Limitations

The present study had several limitations. Most importantly, there is uncertainty regarding the extent to which the findings will generalize to LOAD and to other AD-causing mutations. In addition, the present results are based on a relatively small sample size compared with studies of LOAD. This was especially the case when examining the subsamples of unimpaired and impaired individuals within the mutation carrier group. However, because of the rarity of these mutations, the present sample represents, to our knowledge, one of the largest of its kind with amyloid and tau PET data in carriers of a single ADAD mutation. In addition, it is also important to consider that our findings should be interpreted in the context of the inherent limitations of the techniques used. As such, the temporal differences observed between amyloid and tau pathology in this study may be explained in part by limited detection of pathology by PET methods.

Because age is predictive of clinical onset in the *PSEN1* E280A mutation kindred, cross-sectional assessments across a wide age range in this well-defined cohort are perhaps analogous to what might be expected from the assessment of longitudinal trajectories of biomarker change. However, larger cross-sectional and longitudinal studies are needed to characterize the trajectory of biomarker changes from preclinical to clinical stages.

Conclusions

The present findings add to the growing evidence that molecular markers can characterize biological changes associated with AD in individuals who are still cognitively unimpaired. They also suggest that tau PET imaging may be useful as a biomarker to distinguish individuals at high risk to develop the clinical symptomatology of AD, track progression of the disease, and evaluate response to disease-modifying treatments. In addition, this study confirms that clinical symptoms have a greater association with tau pathology than with amyloid pathology. These findings will inform ongoing preclinical trials with ADAD, such as the Alzheimer Prevention Initiative treatment trial of an A β -modifying agent.³⁵

ARTICLE INFORMATION

Accepted for Publication: August 31, 2017.

Published Online: February 12, 2018.
doi:10.1001/jamaneurol.2017.4907

Author Affiliations: Massachusetts General Hospital, Harvard Medical School, Boston (Quiroz, Sperling, Norton, Cosio, Schultz, Lapoint,

Guzman-Velez, Johnson); Grupo de Neurociencias, Universidad de Antioquia, Medellín, Antioquia, Colombia (Quiroz, Baena, Lopera); Athinoula A. Martinos Center for Biomedical Imaging, Charlestown, Massachusetts (Sperling, Schultz, Lapoint); Brigham and Women's Hospital, Harvard Medical School, Boston, Massachusetts (Sperling, Johnson); Schepens Eye Research Institute of Massachusetts Eye and Ear, Harvard Medical School, Boston (Arboleda-Velasquez, Kim); Department of Brain and Cognitive Sciences, Massachusetts Institute of Technology, Cambridge (Cosio); Massachusetts Eye and Ear, Harvard Medical School, Boston (Miller, Kim); Banner Alzheimer's Institute, Phoenix, Arizona (Chen, Tariot, Reiman).

Author Contributions: Dr Quiroz had full access to all the data in the study and takes responsibility for the integrity of the data and the accuracy of the data analysis.

Study concept and design: Quiroz, Sperling, Lopera, Reiman, Johnson.

Acquisition, analysis, or interpretation of data:

Quiroz, Norton, Baena, Arboleda-Velasquez, Cosio, Schultz, LaPoint, Guzman-Velez, Miller, Kim, Chen, Tariot, Lopera, Reiman, Johnson.

Drafting of the manuscript: Quiroz.

Critical revision of the manuscript for important intellectual content: All authors.

Statistical analysis: Quiroz, Norton, Cosio, Chen, Johnson.

Obtained funding: Quiroz, Arboleda-Velasquez, Reiman, Johnson.

Administrative, technical, or material support: Sperling, Norton, Schultz, LaPoint, Kim, Chen, Tariot, Lopera, Johnson.

Study supervision: Quiroz, Sperling, Kim, Reiman, Johnson.

Conflict of Interest Disclosures: Dr Quiroz was supported by grants 1200-228010 and 1200-228767 from the Massachusetts General Hospital Executive Committee on Research. Dr Sperling receives research support from grants U01 AG032438, U01 AG024904, R01 AG037497, R01 AG034556, and U19 AG010483 from the National Institutes of Health. She is a site principal investigator or coinvestigator for Avid, Bristol-Myers Squibb, Pfizer, and Janssen Alzheimer Immunotherapy clinical trials. Dr Tariot has provided consulting services for Abbott Laboratories, AbbVie, AC Immune, Boehringer-Ingelheim, California Pacific Medical Center, Chase Pharmaceuticals, CME Inc, Medavante, Otsuka, Sanofi-Aventis, Eli Lilly and Company, AstraZeneca, Avanir, Bristol-Myers Squibb, Cognoptix, Janssen, Merck and Company, and Roche; has received research support from AstraZeneca, Avanir, Bristol-Myers Squibb, Cognoptix, Janssen, Merck and Company, Roche, Baxter, Functional Neuromodulation, GE Healthcare, Genentech, Pfizer, Targacept, Avid Radiopharmaceuticals, the National Institute on Aging, and the Arizona Department of Health Services; owns stock options in Adams Pharmaceuticals; and has contributed to a patent for biomarkers of Alzheimer disease owned by the University of Rochester. Dr Reiman has received research funding from AVID and has served as a paid consultant for Eli Lilly. Dr Johnson has provided consulting services for Lilly, Novartis, Janssen, Roche, Piramal, GE Healthcare, Siemens, ISIS Pharma, AZTherapy, and Biogen; has received support from a joint National Institutes of

Health- and Lilly-sponsored clinical trial (Anti-Amyloid Treatment in Asymptomatic Alzheimer's [A4] Study); and has received research support from the National Institute on Aging (grants U19AG10483 and U01AG024904-S1), Fidelity Biosciences, the Michael J. Fox Foundation, and the Alzheimer's Association. No other disclosures were reported.

Funding/Support: This study was supported by grant DP5OD019833 from the National Institutes of Health Office of the Director (Dr Quiroz), the Clafin Distinguished Scholar Award from the Massachusetts General Hospital Executive Committee on Research (Dr Quiroz), the Physician/Scientist Development Award from the Massachusetts General Hospital (Dr Quiroz), the Grimshaw-Gudewicz Charitable Foundation (Drs Arboleda-Velasquez, Miller, and Kim), grants R01 AG046396, R01 AG027435, P50 AG00513421, and P01 AG036694 (Drs Sperling and Johnson) and grant K24 AG035007 (Dr Sperling) from the National Institute on Aging, project 111565741185 from the Administrative Department of Science, Technology, and Innovation (Colciencias Colombia) (Dr Lopera), Fidelity Biosciences (Dr Johnson), Harvard Neurodiscovery Center (Dr Johnson), the Alzheimer's Association (Dr Johnson), and the Marr Foundation (Drs Sperling and Johnson).

Role of the Funder/Sponsor: The funders had no role in the design and conduct of the study; collection, management, analysis, and interpretation of the data; preparation, review, or approval of the manuscript; and decision to submit the manuscript for publication.

Additional Contributions: We thank the *PSEN1* Colombian families for contributing their valuable time and effort, without which this study would not have been possible. We thank the research assistants Madelyn Gutierrez, BA, Lina Velilla, BA, Carolina Ospina, MD, Jorge Rendón, BA, Alex Navarro, BS, and Francisco Piedrahita, BS (Grupo de Neurociencias, Universidad de Antioquia, Medellín, Antioquia, Colombia), for their help coordinating study visits in Colombia. We thank undergraduate students Jairo Martínez and Andrea Ovalle, research assistants Valentina Gaviria, BA, Victoria Jonas, BS, Catherine Munro, BS, Emily Kilpatrick, BS, Nicholas Andrea, BS, Christopher Lee, BS, and David Jin, BS, and Rodrigo Camargo, PhD (Massachusetts General Hospital, Boston), for their help coordinating visits and neuroimaging examinations in Boston. We thank Vivek Devadas, BS (Banner Alzheimer's Institute, Phoenix, Arizona), for his assistance with figures. None of the contributors were compensated for their work.

REFERENCES

1. Iqbal K, Grundke-Iqbal I. Neurofibrillary pathology leads to synaptic loss and not the other way around in Alzheimer disease. *J Alzheimers Dis*. 2002;4(3):235-238.
2. Crews L, Masliah E. Molecular mechanisms of neurodegeneration in Alzheimer's disease. *Hum Mol Genet*. 2010;19(R1):R12-R20.
3. Arnold SE, Hyman BT, Flory J, Damasio AR, Van Hoesen GW. The topographical and neuroanatomical distribution of neurofibrillary tangles and neuritic plaques in the cerebral cortex of patients with Alzheimer's disease. *Cereb Cortex*. 1991;1(1):103-116.

4. Braak H, Braak E. Neuropathological staging of Alzheimer-related changes. *Acta Neuropathol*. 1991; 82(4):239-259.

5. Lopera F, Ardilla A, Martínez A, et al. Clinical features of early-onset Alzheimer disease in a large kindred with an E280A presenilin-1 mutation. *JAMA*. 1997;277(10):793-799.

6. Fleisher AS, Chen K, Quiroz YT, et al. Associations between biomarkers and age in the presenilin 1 E280A autosomal dominant Alzheimer disease kindred: a cross-sectional study. *JAMA Neurol*. 2015;72(3):316-324.

7. Reiman EM, Quiroz YT, Fleisher AS, et al. Brain imaging and fluid biomarker analysis in young adults at genetic risk for autosomal dominant Alzheimer's disease in the presenilin 1 E280A kindred: a case-control study. *Lancet Neurol*. 2012;11(12):1048-1056.

8. Bateman RJ, Xiong C, Benzinger TL, et al. Dominantly Inherited Alzheimer Network. Clinical and biomarker changes in dominantly inherited Alzheimer's disease. *N Engl J Med*. 2012;367(9):795-804.

9. Acosta-Baena N, Sepulveda-Falla D, Lopera-Gómez CM, et al. Pre-dementia clinical stages in presenilin 1 E280A familial early-onset Alzheimer's disease: a retrospective cohort study. *Lancet Neurol*. 2011;10(3):213-220.

10. Quiroz YT, Schultz AP, Chen K, et al. Brain imaging and blood biomarker abnormalities in children with autosomal dominant Alzheimer disease: a cross-sectional study. *JAMA Neurol*. 2015; 72(8):912-919.

11. Johnson KA, Schultz A, Betensky RA, et al. Tau positron emission tomographic imaging in aging and early Alzheimer disease. *Ann Neurol*. 2016;79(1):110-119.

12. Albert MS, DeKosky ST, Dickson D, et al. The diagnosis of mild cognitive impairment due to Alzheimer's disease: recommendations from the National Institute on Aging-Alzheimer's Association workgroups on diagnostic guidelines for Alzheimer's disease. *Alzheimers Dement*. 2011;7(3):270-279.

13. Aguirre-Acevedo DC, Gómez RD, Moreno S, et al. Validity and reliability of the CERAD-Col neuropsychological battery [in Spanish]. *Rev Neurol*. 2007;45(11):655-660.

14. Yesavage JA. Opportunities for and obstacles to treatments for dementias. *J Am Geriatr Soc*. 1983; 31(1):59-60.

15. Reisberg B. Functional Assessment Staging (FAST). *Psychopharmacol Bull*. 1988;24(4):653-659.

16. Shoup TM, Yokell DL, Rice PA, et al. A concise radiosynthesis of the tau radiopharmaceutical, [(18)F]T807. *J Labelled Comp Radiopharm*. 2013;56(14):736-740.

17. Becker JA, Hedden T, Carmasin J, et al. Amyloid- β associated cortical thinning in clinically normal elderly. *Ann Neurol*. 2011;69(6):1032-1042.

18. Braak H, Rüb U, Schultz C, Del Tredici K. Vulnerability of cortical neurons to Alzheimer's and Parkinson's diseases. *J Alzheimers Dis*. 2006;9(3, suppl):35-44.

19. Braak H, Braak E. Diagnostic criteria for neuropathologic assessment of Alzheimer's disease. *Neurobiol Aging*. 1997;18(4, suppl):S85-S88.

20. Chien DT, Bahri S, Szardenings AK, et al. Early clinical PET imaging results with the novel PHF-tau radioligand [F-18]-T807. *J Alzheimers Dis*. 2013;34(2):457-468.
21. Wang L, Benzinger TL, Su Y, et al. Evaluation of tau imaging in staging Alzheimer disease and revealing interactions between β -amyloid and tauopathy. *JAMA Neurol*. 2016;73(9):1070-1077.
22. Logan J, Fowler JS, Volkow ND, et al. Graphical analysis of reversible radioligand binding from time-activity measurements applied to [N-11C-methyl]-(-)-cocaine PET studies in human subjects. *J Cereb Blood Flow Metab*. 1990;10(5):740-747.
23. Amariglio RE, Mormino EC, Pietras AC, et al. Subjective cognitive concerns, amyloid- β , and neurodegeneration in clinically normal elderly. *Neurology*. 2015;85(1):56-62.
24. Hedden T, Van Dijk KR, Becker JA, et al. Disruption of functional connectivity in clinically normal older adults harboring amyloid burden. *J Neurosci*. 2009;29(40):12686-12694.
25. Mormino EC, Betensky RA, Hedden T, et al. Synergistic effect of β -amyloid and neurodegeneration on cognitive decline in clinically normal individuals. *JAMA Neurol*. 2014;71(11):1379-1385.
26. Sperling RA, Johnson KA, Doraiswamy PM, et al; AV45-A05 Study Group. Amyloid deposition detected with florbetapir F 18 ((18)F-AV-45) is related to lower episodic memory performance in clinically normal older individuals. *Neurobiol Aging*. 2013;34(3):822-831.
27. Lippa CF, Saunders AM, Smith TW, et al. Familial and sporadic Alzheimer's disease: neuropathology cannot exclude a final common pathway. *Neurology*. 1996;46(2):406-412.
28. Sepulveda-Falla D, Matschke J, Bernreuther C, et al. Deposition of hyperphosphorylated tau in cerebellum of PS1 E280A Alzheimer's disease. *Brain Pathol*. 2011;21(4):452-463.
29. Fleisher AS, Chen K, Quiroz YT, et al. Florbetapir PET analysis of amyloid- β deposition in the presenilin 1 E280A autosomal dominant Alzheimer's disease kindred: a cross-sectional study. *Lancet Neurol*. 2012;11(12):1057-1065.
30. Fleisher AS, Chen K, Liu X, et al. Using positron emission tomography and florbetapir F18 to image cortical amyloid in patients with mild cognitive impairment or dementia due to Alzheimer disease. *Arch Neurol*. 2011;68(11):1404-1411.
31. Benzinger TL, Blazey T, Jack CR Jr, et al. Regional variability of imaging biomarkers in autosomal dominant Alzheimer's disease. *Proc Natl Acad Sci U S A*. 2013;110(47):E4502-E4509.
32. Jack CR Jr, Knopman DS, Jagust WJ, et al. Tracking pathophysiological processes in Alzheimer's disease: an updated hypothetical model of dynamic biomarkers. *Lancet Neurol*. 2013;12(2):207-216.
33. Benzinger TLS, Gordon BA, Friedrichsen KA, et al; Dominantly Inherited Alzheimer Network (DIAN) Study Group. Tau PET imaging with AV-1451 in autosomal dominant Alzheimer's disease: update from the Dominantly Inherited Alzheimer Network (DIAN). *Alzheimers Dement*. 2016;12(7, suppl):378. doi:10.1016/j.jalz.2016.06.709
34. Benzinger T, Friedrichsen K, Sul Y, et al. Patterns of tau deposition using [18F]-AV-1451 in autosomal dominant Alzheimer's disease: results from the DIAN. Paper presented at: Human Amyloid Imaging 2016; January 14, 2016; Miami, FL.
35. Reiman EM, Langbaum JB, Fleisher AS, et al. Alzheimer's Prevention Initiative: a plan to accelerate the evaluation of presymptomatic treatments. *J Alzheimers Dis*. 2011;26(suppl 3):321-329.